ISSN 1063-7397, Russian Microelectronics, 2015, Vol. 44, No. 3, pp. 190–196. © Pleiades Publishing, Ltd., 2015.
Original Russian Text © B.G. Konoplev, E.A. Ryndin, M.A. Denisenko, 2015, published in Mikroelektronika, 2015, Vol. 44, No. 3, pp. 220–227.

Components of Integrated Microwave Circuits Based on Complementary Coupled Quantum Regions

B. G. Konoplev, E. A. Ryndin, and M. A. Denisenko
Southern Federal University, ul. Bol'shaya Sadovaya 105/42, Rostov-on-Don, 344006 Russia
e-mail: rynenator@gmail.com
Received July 10, 2014

Abstract—A method for the design of high-speed components of integrated circuits based on III–V semiconductors using complementary logic principles, which provides an increase in performance and degree of integration of microwave integrated circuits, is considered.

DOI: 10.1134/S1063739715030051

Components of modern microwave integrated circuits (ICs) are based on high-speed heterojunction transistor structures (MESFET, HEMT, VMT), which are characterized by operational frequencies of up to hundreds of gigahertz and are implemented based on III–V semiconductors. At the same time, the use of heterostructures with solely electron conduction in microwave devices has led to the increased switching energy of integrated components and has restricted the degree of integration of microwave ICs [1, 2].

This problem is successfully resolved in silicon-based integrated electronics by using the complementary logic principles. However, due to the fact that the hole mobility in III–V semiconductors is lower than the electron mobility by a factor of several tens [2], the use of integrated components based on transistor structures with mutually complementary conduction types in microwave ICs is considered inappropriate.

This study is aimed at the development of the design method of high-speed components of ICs based on III–V semiconductors using the complementary logic principles, which improves the performance and degree of integration of microwave ICs.

The main notions of the proposed design method of high-speed components of ICs based on III–V semiconductors using the complementary logic principles can be shortly formulated as follows:

(i) The integrated components are constructed based on nanoheterostructures containing coupled quantum regions with mutually complementary conduction types;

(ii) Each of the coupled quantum regions of a definite conduction type borders heavily doped semiconductor regions of ohmic contacts, by means of which the electric field is formed, which provides the conditions for the longitudinal transport of charge carriers in quantum regions, and the state of the coupled quantum regions and integrated component in general is registered;

(iii) Each nanoheterostructure with the coupled quantum regions with electron and hole conduction contains one or several pairs of controlling transitions (the Schottky transitions and *p-n* junctions), by means of which the transverse electric field, which controls the state of the coupled quantum regions and integral component in general, is formed;

(iv) The variation in the direction of the transverse controlling field leads to the relocation of density maxima of carriers (electrons and holes) into one of the coupled quantum regions of the corresponding conduction type, which provides the variation in the conductivity ratios of the coupled quantum regions and, consequently, the variation in the state of the integrated component. The delay time of the integrated component is determined by the lag of the transverse carrier's relocation in the quantum regions and is not limited by the carrier's flight time (transverse transport time) in the active region of the nanoheterostructure, which levels the switching time of the nanostructures with the electron and hole conduction despite the considerable difference in the electron and hole mobilities in III–V semiconductor materials;

(v) The variation in the transverse controlling field is fulfilled so that the total number of carriers in the coupled quantum regions in any conduction type remain almost invariable during the relocation of the maxima of the electron and hole density in any state of the integrated component. If this requirement is fulfilled, the delay time of the integrated component is not limited by the comparatively inertial accumulation and forcing-out of the mobile carriers in the active region;

(vi) In correspondence with the complementary logic principles, the integrated components are designed based on pairs of coupled quantum regions with the electron and hole conduction controlled by common controlling voltages and are characterized by antiphase variations in conductivity, which provide the

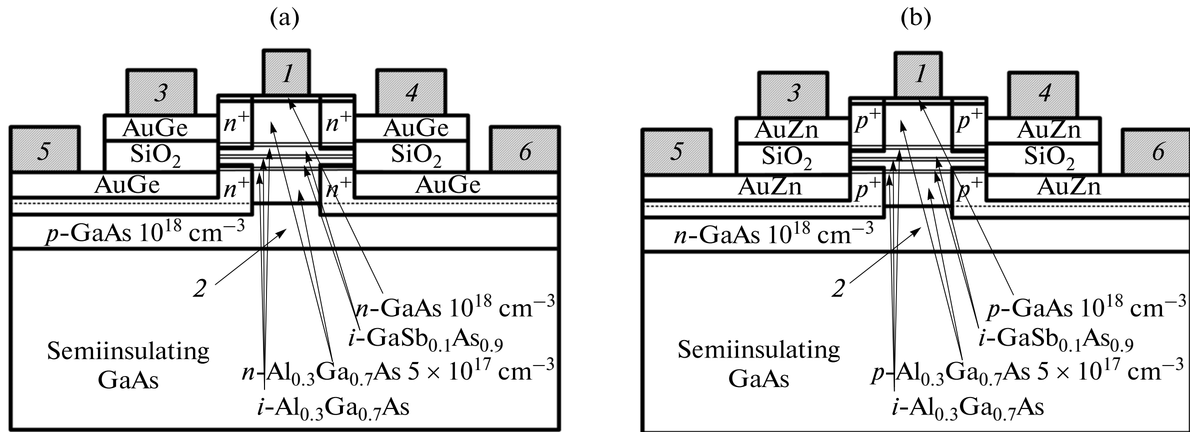

Fig. 1. Nanostructures with the tunnel-coupled channel-wells with (a) electron and (b) hole conduction types (*1*, *2* are controlling contacts and *3–6* are ohmic contacts to quantum well channels) [3].

minimization of through currents in steady states and during switching, considerably lowering the switching energy of the components and consumed power of the integrated circuit as a whole;

(vii) The function of the integrated component is determined by the connection variant of heavily doped regions of ohmic contacts of the coupled quantum states and controlling contacts;

(viii) Allowing for the significant mobility ratio of electrons and holes in III–V semiconductors, conductivity leveling in the open quantum region of the conduction band and valence band enriched by carriers is a serious problem. This problem is solved in terms of the proposed methodology by the band engineering methods—the use of heterojunctions with valence band discontinuities exceeding the conduction band discontinuities, which provides an increase in the hole concentration in the quantum regions of the valence band compared to the electron concentration in the quantum regions of the conduction band and, correspondingly, resistivity leveling in these regions when the carrier density maxima in them are relocated.

Figure 1 schematically shows the nanostructures with $GaAs/Al_{0.3}Ga_{0.7}As/GaSb_{0.1}As_{0.9}$ heterojunctions, which contain tunnel-coupled quantum well channels with the electron and hole conduction types—the tunnel-coupled nanostructures (TCNs). They can be used as a base for the functionally different integrated components: logic, commuting, memory cells, etc. [3].

The TCN of a definite conduction type is based on two ($GaSb_{0.1}As_{0.9}$) quantum wells, which are separated by the $Al_{0.3}Ga_{0.7}As$ tunnel-transparent heterobarrier and have separate ohmic contracts (*3*, *4* and *5*, *6* in Fig. 1) for registration of the state of the quantum system. The antiphase control over the tunnel relocation of the carrier density maxima between the coupled quantum wells is performed by means of the Schottky gate *1* and controlling *p-n* junction *2* at the interface with the semiinsulating substrate as shown in Fig. 1 [3]. Controlling *p-n* junctions are fulfilled using *n*-GaAs and *p*-GaAs hidden epitaxial layers. Ohmic contacts to the regions of controlling *p-n* junctions *2* are fulfilled at the periphery of the tunnel-coupled nanostructures and are not shown in Fig. 1. The n/p-$Al_{0.3}Ga_{0.7}As$ doped barrier regions are separated from the quantum wells by the i-$Al_{0.3}Ga_{0.7}As$ undoped spacers to weaken the scattering of the mobile carriers during their longitudinal transport in the quantum channels across the Coulomb long-range potential of impurity ions in the barrier regions. The mutual isolation of tunnel-coupled nanostructures on the crystal is performed by means of the semiinsulating substrate and periphery amorphization regions of epitaxial layers with boron or etching of the mesa regions. The metallized connections between the TCN are fulfilled according to the component circuits depending on the functional indentation of the integrated components. The circuits of the inverter, the 2NAND/2NOR gates, bilateral switch, and static memory cell are based on complementary TCNs.

Tunnel-coupled quantum well channels are conventionally shown in the circuits presented in Fig. 2 in the form of transistors of the corresponding conduction type connected by dotted lines due to the absence of the standard circuit notation [4, 5].

In order to implement the complementary logic principles in integrated components based on the tunnel-coupled nanostructures with the complementary conduction types, whose circuits are presented in Fig. 2, the concept of antiphase input and output signals is used: according to Fig. 2a, two inverters operating in the antiphase are implemented based on two TCNs with complementary conduction types; according to Fig. 2b, when implementing NAND logic gates in the antiphase part of components, the tunnel-coupled channels are connected by the NOR circuit; and

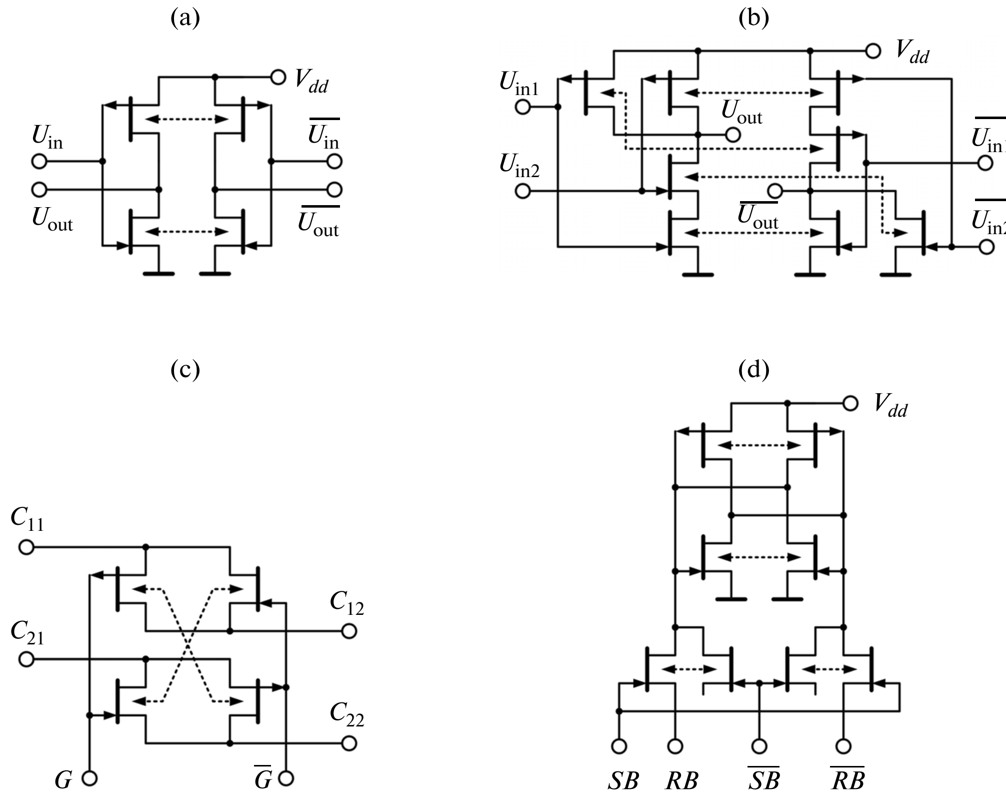

Fig. 2. Circuits of (a) inverter, (b) 2NAND/2NOR component, (c) bilateral switch, and (d) static memory cell based on the complementary TCNs.

according to Fig. 2c, two bilateral switches controlled by signals G and operating in the antiphase are implemented based on two complementary TCNs. The concept of antiphase signals requires twice as many channels to implement the logic functions compared, for example, with the silicon components based on the complementary logic principles. However, the use of vertical integration in the TCN approximately halves the area occupied by components on the crystal compared with the planar arrangement of quantum well channels [4].

In some cases, in order to decrease the area occupied by the integrated components of the crystal, improve their performance, and widen their functional possibilities, design-manufacturing variants of nanostructures based on the coupled quantum regions with the complementary conduction types differing from those presented in Figs. 1 and 2 can be implemented in terms of the proposed methodology. For example, high-speed bilateral switches can be implemented based on functionally integrated nanostructures with combined quantum regions without tunnel heterojunction barriers separating the quantum well channels. The nanostructures of four-contact and eight-contact bilateral switches based on the combined quantum regions with the electron and hole conduction and the circuits of these integrated components are presented in Figs. 3 and 4, respectively [5, 6].

The tunnel heterobarriers are absent in these integrated switches, while the relocation of the density maxima of the electrons and holes in each of the combined quantum regions is controlled by four or eight controlling junctions: by two (G_1, G_2 in Fig. 3) or by four (G_1–G_4 in Fig. 4) Schottky junctions at the upper boundary and, correspondingly, by two (G_3, G_4 in Fig. 3) or by four (G_5–G_8 in Fig. 4) controlling p-n junctions at the interface with the semiinsulating substrate, which makes it possible to perform the bilateral commutation of any pair of four contacts C_1–C_4 in Fig. 3 or any pair (or quad) of eight contacts C_1–C_8 in Fig. 4. The switch functioning presented in Fig. 3 is illustrated by the table in which the combination of the logic levels of the controlling voltages and corresponding commuting groups of contacts are presented.

According to the structures and circuits of the switches presented in Figs. 3 and 4, the nanostructure with the combined quantum region of a definite conduction type, when performing the functions of four-transistor or eight-transistor circuit, occupies an area on the crystal approximately equal to the area of one dual-gate transistor and provides an increase in efficiency of using the crystal area by a factor of 3–6 compared to analogs based on the traditional integrated transistors, due to its three-dimensional functional integration [5, 6].

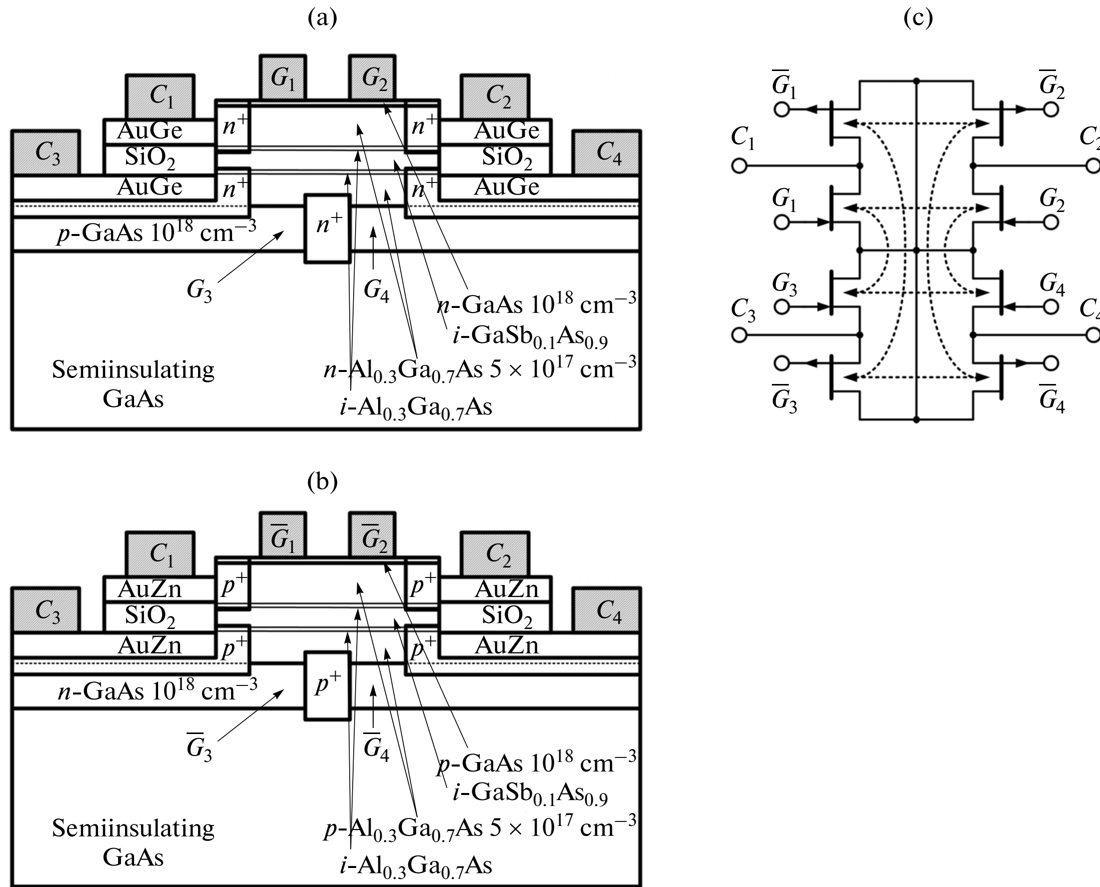

Fig. 3. Four-contact bilateral switch based on the coupled quantum regions: nanostructures with (a) electron and (b) hole conduction; (c) switch circuit.

It should be noted that the absence of tunnel barriers in coupled quantum regions would definitely undesirably lower the ratio of currents flowing through the connected and disconnected contact groups. This conclusion is confirmed by the results of numerical modeling of the four-contact switch presented in [5], according to which, carrier concentrations in the enrichment zones of the coupled quantum regions can exceed the carrier concentrations in the depletion regions only by 1–3 orders of magnitude, which should be taken into account when developing integrated switches with coupled quantum regions and devices based on them.

The principles of the controlled relocation of carrier density maxima in the coupled quantum regions with the complementary conduction types, which are laid into the basis of the methodology under consideration, can be also used to implement the microelec-

Combinations of logic levels of controlling voltages of the four-contact switch and the corresponding commuted groups of contacts

Ordinal no.	Logic levels at controlling inputs				Commuted group of contacts
	G_1	G_2	G_3	G_4	
1	0	0	1	1	C_3, C_4
2	1	1	0	0	C_1, C_2
3	0	1	0	1	C_2, C_4
4	1	0	1	0	C_1, C_3
5	0	1	1	0	C_2, C_3
6	1	0	0	1	C_1, C_4

The notation presented in the table corresponds to Fig. 3.

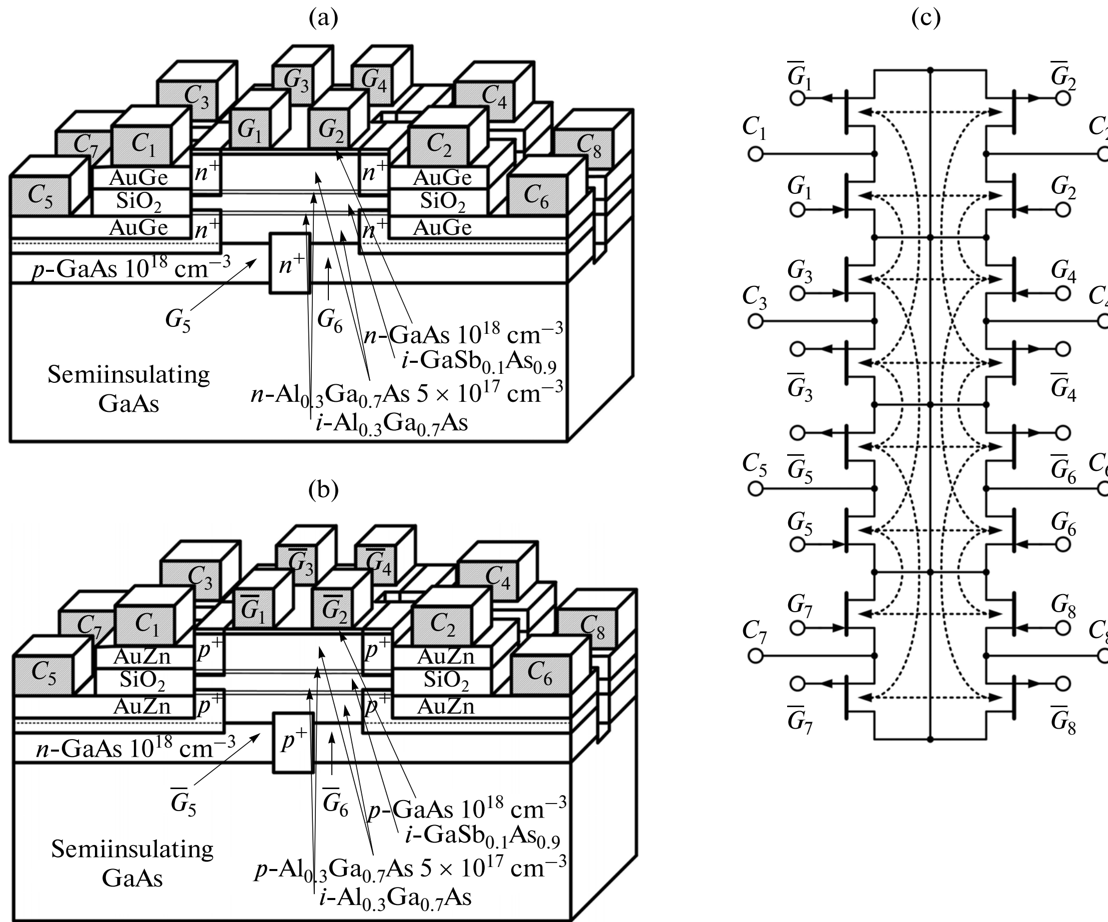

Fig. 4. Eight-contact bilateral switch based on the coupled quantum regions: nanostructures with (a) electron and (b) hole conduction; (c) switch circuit.

tronics components, particularly, injection lasers and optical emission modulators, which are widely used in integrated optoelectronic systems to convert electrical signals into optical ones [7–11].

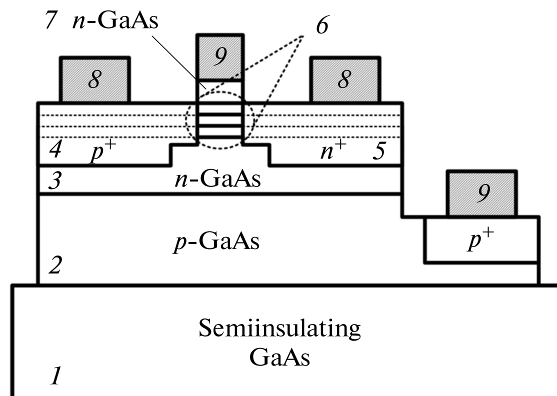

Fig. 5. Structure of a functionally integrated injection laser-modulator: (*1*) semiinsulating GaAs substrate, (*2*) *p*-GaAs, (*3*, *7*) *n*-GaAs, (*4*, *5*) *p*+ and *n*+ regions, (*6*) nanoheterostructure of the optical radiation modulator, (*8*) supply contacts, and (*9*) controlling contacts.

Currently, polarization modulators based on the electrooptical or magnetooptical effect are successfully used for the external modulation of laser radiation [12]. However, their substantial disadvantage, which is especially critical in the region of integrated microelectronics, is the use of such crystalline materials as, for example, lithium niobate ($LiNbO_3$), which leads to the impossibility of fabricating modulators in a single production cycle with semiconductor integrated components. With the internal modulation by means of controlling the laser pumping current, the dynamics of emission modulation are determined by the transient processes in the supply circuit and the inertness of the carrier accumulation and escape in the active laser region. Due to this, the maximal modulation frequency of the optical radiation does not exceed tens of gigahertz [12].

The design method of injection lasers with the functionally integrated modulators proposed in this methodology is directed to an increase in modulation frequencies of the optical radiation and attainment of

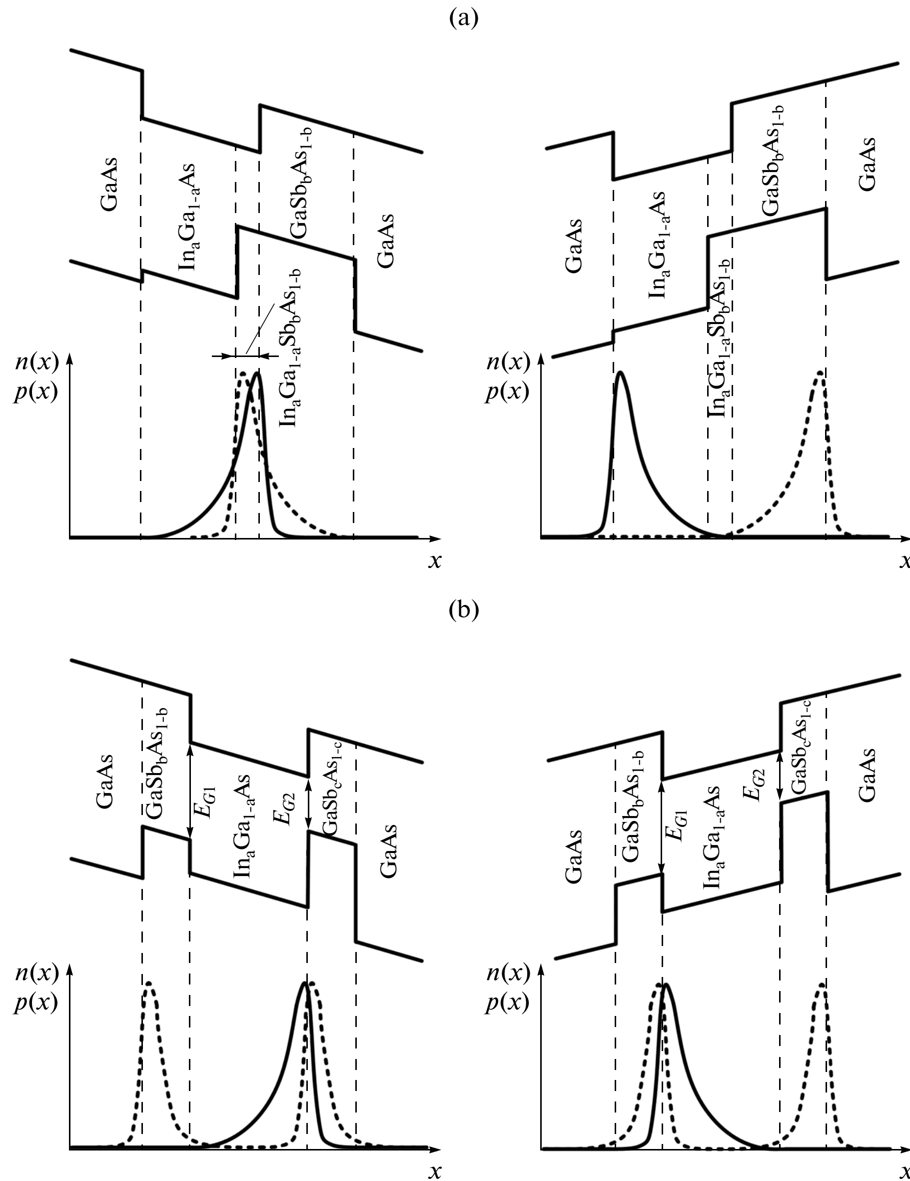

Fig. 6. Band diagrams and concentration distributions of electrons ($n(x)$—solid lines) and holes ($p(x)$—dotted lines) in injection laser-modulators with the (a) amplitude and (b) frequency modulation of optical radiation.

the manufacturing compatibility of lasers and modulators with integrated components. This method consists of the following points:

(i) the injection laser-modulator is a semiconductor nanoheterostructure, the generalized variant of which is schematically shown in Fig. 5, in which the p+ and n+ regions (items *4*, *5* in Fig. 5) with the corresponding ohmic (supplying) contacts (item *8* in Fig. 5) and regions of the amplitude or frequency modulator with additional (controlling) contacts (item *9* in Fig. 5) and controlling junctions (the Schottky junction—items *7*, *9* and p-n junction—items *2*, *3* in Fig. 5) are functionally integrated in the form of definitely configured system of quantum wells *6* [13];

(ii) a definite pumping current providing the inverse population and summary number of electrons and holes in the quantum wells of the active region invariable in time (item *6* in Fig. 5) is specified in the laser supply circuit (item *8* in Fig. 5);

(iii) to perform the internal modulation, i.e., the modulation of the laser beam during its formation, quantum wells of the conduction band in the modulator nanoheterostructure (item *6* in Fig. 5), which is functionally integrated into the injection laser, are spatially shifted relative to the quantum wells of the valence band by using second-type heterojunctions. The band diagrams and distributions of the carrier concentration in the nanostructures of the amplitude

and frequency modulators under opposite directions of the controlling field are presented in Fig. 6. The relocation and spatial superposition of the density maxima of the electrons and holes in the quantum wells of the conduction band and valence band, which leads to an increase in the laser radiation intensity, is observed in the amplitude modulator (Fig. 6a) for one direction of the controlling field; and the inverse relocation and, correspondingly, the spatial separation of the density maxima of the electrons and holes in the quantum wells, which leads to a decrease in the intensity of the generated radiation, are observed with the opposite direction of the controlling field. The spatial superposition of the density maxima of the electrons and holes in the quantum wells separated by the forbidden band with width E_{G1} and generation of the laser radiation with wavelength λ_1 are observed in the nanoheterostructure of the frequency modulator (Fig. 6b) for one direction of the controlling field; and the spatial superposition of the density maxima of the electrons and holes in the quantum wells separated by the band gap with width E_{G2} and, correspondingly, the generation of a laser radiation with wavelength λ_2, are observed for the opposite direction of the controlling field;

(iv) if the injection level of the electrons and holes into the active laser region is invariable, the summary carrier number in the quantum wells remains almost invariable upon varying the controlling field direction, due to which, the maximal modulation frequency of the laser beam is determined by the time of the field-controlled relocation of the density maxima of the electrons and holes in the quantum regions of the conduction band and valence band rather than by the relatively inertial carrier accumulation and escape processes in the active laser region;

(v) allowing for the fact that the optical radiation spectrum of a functionally integrated laser-modulator in the case of the frequency modulation contains the emission maxima at wavelengths λ_1 and λ_2, the resonator length should be simultaneously a multiple of $\lambda_1/2$ and $\lambda_2/2$ [7–11].

According to the results of the numerical modeling the integrated components based on the coupled quantum regions with the complementary conduction types presented in [4, 5, 7, 14, 15], the minimal delay time of the components is determined by the inertness of the controlled relocation of the density maxima of the mobile carriers under the effect of the transverse controlling field and reaches $(1.3–0.8) \times 10^{-13}$ s, which corresponds to the frequencies of the terahertz range.

ACKNOWLEDGMENTS

This study was supported by the Russian Foundation for Basic Research, project nos. 13-07-00274 and 14-07-31234; and by the Ministry of Education and Science of the Russian Federation, project no. 8.797.2014K.

REFERENCES

1. Kallfass, I., Pahl, P., Massler, H., Leuther, A., Tessmann, A., Koch, S., and Zwick, T., A 200 GHz monolithic integrated power amplifier in metamorphic HEMT technology, *IEEE Microwave Wireless Comp. Lett.*, 2009, vol. 19, no. 6, pp. 410–412.
2. Pala, N., Hu, X., Deng, J., Yang, J., Gask, R., Yang, Z., Koudymov, A., Shur, M.S., and Simin, G., Drain-to-gate field engineering for improved frequency response of GaN-based HEMTs, *Solid-State Electron.*, 2008, no. 52, pp. 1217–1220.
3. Konoplev, B.G. and Ryndin, E.A., RF Patent, no. 2287896, 2006.
4. Konoplev, B.G. and Ryndin, E.A., Integral logic components based on tunnel-coupled nanostructures, *Izv. Vyssh. Uchebn. Zaved., Elektronika*, 2006, no. 3, pp. 18–26.
5. Ryndin, E.A., Ultrahigh-speed electron switches based on the controlled relocation of the maximum of the carrier wave function, *Vestn. Yuzhn. Nauch. Tsentra Ross. Akad. Nauk*, 2006, vol. 2, no. 2, pp. 8–16.
6. Konoplev, B.G. and Ryndin, E.A., RF Patent, no. 2304825, 2007.
7. Konoplev, B.G., Ryndin, E.A., and Denisenko, M.A., Integrated injection laser with the controlled relocation of the amplitude maximum of carrier wave functions, *Vestn. Yuzhn. Nauch. Tsentra Ross. Akad. Nauk,* 2010, vol. 6, no. 3, pp. 5–11.
8. Konoplev, B.G., Ryndin, E.A., and Denisenko, M.A., Injection laser with a functionally integrated frequency modulator based on spatially shifted quantum wells, *Tech. Phys. Lett.*, 2013, vol. 39, no. 11, pp. 986–989.
9. Ryndin, E.A. and Denisenko, M.A., A functionally integrated injection laser-modulator with the radiation frequency modulation, *Russ. Microelectron.*, 2013, vol. 42, no. 6, pp. 360–362.
10. Konoplev, B.G., Ryndin, E.A., and Denisenko, M.A., An injection laser with a functionally integrated frequency modulator based on spatially shifted quantum wells, *Pis'ma Zh. Tekh. Fiz.*, 2013, vol. 39, no. 22, pp. 9–16.
11. Ryndin, E.A. and Denisenko, M.A., A functionally integrated injection laser-modulator with the radiation frequency modulation, *Russ. Microelectron.*, 2013, vol. 42, no. 6, p. 360.
12. Malyshev, V.A., *Osnovy kvantovoi elektroniki i lazernoi tekhniki* (Foundations of Quantum Electronics and Laser Technique), Moscow: Vysshaya shkola, 2005.
13. Konoplev, B.G., Ryndin, E.A., and Denisenko, M.A., RF Patent, no. 2400000, 2010.
14. Konoplev, B.G. and Ryndin, E.A., A study of the transport of charge carriers in coupled quantum regions, *Semiconductors*, 2008, vol. 42, no. 13, pp. 1462–1468.
15. Ryndin, E.A. and Denisenko, M.A., A model of functionally integrated injection laser-modulators for integrated circuits of optical commutation, *Izv. Vyssh. Uchebn. Zaved., Elektronika*, 2012, no. 6 (98), pp 26–35.

Translated by N. Korovin